

PART SEVEN

THEORETICAL SEISMIC SIGNAL SOURCE
AND TRANSMISSION CHARACTERISTICS

PART SEVEN

THEORETICAL SEISMIC SIGNAL SOURCE
AND TRANSMISSION CHARACTERISTICS

TABLE OF CONTENTS

| | <u>Page</u> |
|--------------------------------------------------------------------------------------------|-------------|
| List of Tables | 7.iii |
| List of Figures | 7.iv |
| I. SUMMARY | 7.1 |
| II. INTRODUCTION | 7.2 |
| III. SOURCE STRENGTH AND SOURCE SPECTRUM | 7.2 |
| IV. NATURE OF THE MINER'S SOURCE | 7.9 |
| V. SIGNAL ATTENUATION | 7.12 |
| A. GEOMETRICAL SPREADING | 7.12 |
| B. ENERGY DISSIPATION | 7.12 |
| C. ENERGY PARTITION | 7.14 |
| VI. DISTORTION OF SEISMIC WAVE FRONT FOR AN IMPACT IN A MINE OPENING | 7.17 |
| VII. THEORETICAL ESTIMATION OF THE SIGNAL LEVEL AS A FUNCTION OF RANGE | 7.24 |
| VIII. DEVELOPMENT OF LOW-FREQUENCY SEISMIC SOURCE FOR THE DETECTION OF SURVIVING MINERS | 7.25 |
| IX. FUTURE INVESTIGATIONS | 7.30 |
| X. REFERENCES | 7.31 |
| APPENDIX A - USE OF A COUPLER IN THE CONVERSION OF IMPACT ENERGY INTO SEISMIC ENERGY | 7.32 |
| APPENDIX B - QUADRATURE WEIGHTING METHOD FOR MINER LOCATION ARRAYS | 7.33 |

PART SEVEN

THEORETICAL SEISMIC SIGNAL SOURCE
AND TRANSMISSION CHARACTERISTICS

LIST OF TABLES

| <u>Table No.</u> | <u>Title</u> | <u>Page</u> |
|------------------|-----------------------------------------------------|-------------|
| 1 | Average Values of Q | 7.13 |
| 2 | Q's for Typical Weathering Layers | 7.14 |
| 3 | Average Values of Attenuation Coefficient, α | 7.14 |

PART SEVEN

THEORETICAL SEISMIC SIGNAL SOURCE
AND TRANSMISSION CHARACTERISTICS

LIST OF FIGURES

| <u>Figure No.</u> | <u>Title</u> | <u>Page</u> |
|-------------------|--------------------------------------------------------------------------------------------------------------------------------------------------------------------------------------------------------------------------------------------------------------------------------------------------------------|-------------|
| 1 | The Force Function and the Fourier Transform | 7.6 |
| 2 | Source Impact Spectrum Assumed by Westinghouse | 7.8 |
| 3 | Attenuation Coefficient Versus Frequency with a Low-Frequency Cut-off | 7.13 |
| 4 | Four Incident Plane Waves are Shown Approaching a Plane Interface. Any One of These Produces Four Outgoing Waves, P, S, P', S'. The Angles of Emergence for Shear Waves are σ and σ' , and for Compressional Waves, δ and δ' . The Upper Medium is Unprimed. (After Nafe, 1957). | 7.16 |
| 5 | Fraction of Incident Energy Carried Away in Refracted (P,S) and Reflected (P',S') Waves | 7.18 |
| 6 | Radiation Patterns of a Simple Force in (a) An Infinite Medium and (b) A Mine Opening | 7.19 |
| 7 | Plane Views for Mine Tunnel | 7.20 |
| 8 | Distorted Wave Fronts of a Vertical Section A-A' | 7.21 |
| 9 | Distorted Wave Fronts of a Vertical Section B-B' | 7.22 |
| 10 | Distorted Wave Fronts of a Vertical Section B-B' for an Impact on Rib | 7.23 |
| 11 | Models for Estimating Signal Levels on the Surface | 7.24 |
| 12 | Estimated Peak-to-Peak Vertical Particle Velocity for the First P-Wave Arrival (Based on Theoretical Considerations) | 7.26 |
| 13 | Permanent Installation of a Pendulum | 7.27 |
| 14 | Attenuation of High Frequencies Through Weathering Layers as Deduced from Plots 28 and 39 of Report 8, Copper Queen | 7.28 |

PART SEVEN

THEORETICAL SEISMIC SIGNAL SOURCE
AND TRANSMISSION CHARACTERISTICS

LIST OF FIGURES
(Continued)

| <u>Figure No.</u> | <u>Title</u> | <u>Page</u> |
|-------------------|--------------------------------------------------------------|-------------|
| 15 | Examples of Low Frequency Sources | 7.29 |
| 16 | Repeated Low-Frequency Signals As Received on the Surface | 7.30 |

PART SEVEN

THEORETICAL SEISMIC SIGNAL SOURCE AND TRANSMISSION CHARACTERISTICS

John T. Kuo
Columbia University

I. SUMMARY

The miner's seismic source strength can be approximately estimated on the basis of a single force acting in an infinite medium. Because of the uncertainty involved in estimating the amount of conversion from mechanical energy to seismic energy, the source strength thus estimated may be in error by as much as a half-order of magnitude. Calculations of wave transmission must take into account geometrical spreading, dissipation of energy by internal friction, and energy partition due to reflection and refraction of waves impinging on interfaces in the layered earth.

Theoretically derived peak-to-peak particle velocities in microinches per second (μ IPS) are given for two models; viz: (i) 50-foot thick and (ii) 100-foot thick 4000 ft/sec layers with $Q = 20$, overlying a half-space of 10,000 ft/sec material with $Q = 50$; for the cases of a hammer blow and a timber impact, at the frequencies of 50 Hz and 100 Hz. Comparison of the theoretically derived peak-to-peak particle velocity with experimental data taken at the Copper Queen Mine indicates that the theoretical particle velocity may be overestimated.

A discussion of the distortion of seismic wavefronts by mine tunnels indicates that it is unfavorable to use a seismic source impact on the floor of the tunnel, since deceptive delays in arrival time are liable to occur at the surface.

A program of parallel theoretical and experimental work is required to clarify uncertainties still associated with the nature and strength of the miner's seismic source signal which cannot be resolved within the approximations of this work. Its major components include theoretical investigations of the

- (1) Wave diffraction and scattering of an impact source on a face of a cylindrical cavity.
- (2) Impact of an elastic object on an elastic medium.

Experimental measurements of the signal spectrum under carefully controlled conditions are also necessary in order that the frequency spectrum of the source be determined accurately; it is virtually impossible to determine the source strength near or at the source since the problem of the efficiency of conversion of mechanical to seismic energy is extremely difficult to handle.

For the initial detection of a surviving miner in a disaster struck mine, a "low-frequency" source of considerable strength is desired. It is proposed that experimental efforts be devoted to the development and test of such a source, in conjunction with the concept of a coupler to enhance the conversion of mechanical energy into seismic energy.

II. INTRODUCTION

The thrust of this work is confined to the surface seismic detection and location of trapped miners in a coal mine. It is imperative that the procedure of locating trapped miners be as unsophisticated to operate as is feasible; the final system should ideally be as close to a "push button" type as possible.

The investigation of the problem of the detection and location of a trapped miner starts from the following initial conditions:

- (i) A relatively weak but high-frequency seismic source
- (ii) Seismic-wave transmission in an inhomogeneous medium generally capped by an extremely lossy weathering layer of variable thickness.
- (iii) Relatively high background noise in the frequency band of the signal.
- (iv) Limitations in the resolution of currently employed seismic methods in both the time and frequency domain.

The following analysis is designed to shed light on items (i) and (ii).

The results obtained in this investigation of seismic sources are consistent with being able to detect miners at ranges up to on the order of 1000 feet, and to measure arrival times to within a few milliseconds. Hence under the most favorable signal-to-noise and geological conditions, it is conceivable (see Appendix B) that the location of a miner to within 30 feet should be achieved by seismic means, and a reasonable expectation in a range of situations would be location accuracies to within 100 feet.

III. SOURCE STRENGTH AND SOURCE SPECTRUM

It is reasonably certain that the miner detection and location system has to depend predominantly upon the compressional wave, certainly for location purposes, as neither shear waves nor surface waves offer the necessary resolving power. Suppose that a hammer blow (or a timber impact) on the roof, rib

or floor in a given mine can be approximated by a single force in an infinite medium. Such an approximation is only good for estimating the order of magnitude of the source strength. More precise estimates demand a rigorous theoretical treatment of the problem. Neglecting the distortion of the wave front, due to a system of cavities, which will be discussed in a later section, the radial component of the particle displacement for near-field, as shown by White (1965), is given by

$$u_r = \frac{G \cos \phi}{4\pi\rho r} \left[\frac{1}{V^2} g\left(t - \frac{r}{V}\right) + \frac{2}{rV} g^I\left(t - \frac{r}{V}\right) + \frac{2}{r^2} g^{II}\left(t - \frac{r}{V}\right) \right] \quad (1)*$$

where G is the magnitude of the force, ρ is the density of the medium, V is the compressional wave velocity, and ϕ is the angle between the source and the point of observation with respect to the vertical.

Fortunately, for the present application of Equation (1) to the seismic detection and location of a miner, the distance from the source to the observation point is generally large, in the order of at least several wavelengths, e.g., a frequency of 75 Hz and a velocity of 8000 ft/sec corresponds to a wavelength of 106 feet, whereas the observation point is typically located at least 400 feet away from the source. From that point of view, the first term in the right-hand side of Equation (1) is predominant, as the second and third terms decay very rapidly at large distances. However, the efficiency of the conversion of the mechanical energy into seismic energy at the immediate point of impact is extremely difficult to estimate accurately, as an appreciable amount of energy is dissipated at the point of impact due to fracture and plastic deformation of the rock.

For a crude estimate of the particle displacement at an observation point located sufficiently far away from the source, Equation (1) may be written as

$$u_r \approx \frac{G \cos \phi}{4\pi\rho V^2 r} g\left(t - \frac{r}{V}\right) + O\left(\frac{1}{r^2}\right) \quad (1a)$$

which is also used by Westinghouse (see Westinghouse Final Report (1971),[†] Volume II, p. 78-83). It is possible to extrapolate the particle displacement back to the source in a half-theoretical and half-empirical fashion to obtain values for the source strength and frequency characteristics.

* References to Figures, Tables, and Equations apply to those in this Part unless otherwise noted.

[†] Westinghouse Contract H0101262 with Bureau of Mines.

Introducing the dissipation of energy by internal friction, Equation (1a) may then be written as

$$u_r \approx \frac{G \cos \phi}{4\pi\rho V^2 r} g\left(t - \frac{r}{V}\right) e^{-\alpha r} + O\left(\frac{1}{r^2}\right) \quad (1b)$$

where α is the dissipation coefficient. The radial component of the particle velocity can then be obtained by differentiating Equation (1b), neglecting the terms higher than $1/r^2$.

$$\dot{u}_r \approx \frac{G \cos \phi}{4\pi\rho V^2 r} \dot{g}\left(t - \frac{r}{V}\right) e^{-\alpha r} \quad (2)$$

There is a factor of two increase in the displacement if the detection of the motion is made on the surface of a half-space. In addition, the vertical displacement usually detected is a component of the radial particle displacement so that equation (2) should be multiplied by a factor of $2 \cos \phi$.

Instead of letting the force be of the form

$$g(t) = e^{-t/\tau} \quad (3)$$

as used by Westinghouse, a closer representation of the real source, as recorded through the Westinghouse seismic system, may be given by

$$g(t) = e^{-at} \sin bt. \quad (4)$$

The force function $g(t)$ has the form shown in Figure 1. The integral of the force from a hammer blow or a timber impact is equal to an approximation of an impact of very short duration for the case of an inelastic collision, I , such that

$$I = \int_0^{\infty} Gg(t) dt = Mv \quad (5)$$

where M is the mass of the impact object and v is the impact velocity.

Substituting $g(t)$ from Equation (4) into (5) and solving for G , we have

$$G = Mv \left(\frac{a^2 + b^2}{b} \right) \quad (6)$$

The Fourier Transform of Equation (4) thus gives the spectrum for the impact (a hammer or timber upon the roof, rib or floor) as follows

$$\begin{aligned} G(i\omega) &= \int_0^{\infty} e^{-at} \sin bt e^{-i\omega t} dt \\ &= \frac{b(a^2 + b^2 - \omega^2 - 2i\omega a)}{(a^2 + b^2 - \omega^2)^2 + 4\omega^2 a^2} \end{aligned} \quad (7)$$

Assuming that $a = \frac{b}{n}$ where n is either an integer or a non-integer, equations (6) and (7) become, respectively

$$G = \frac{Mv (n^2 + 1) b}{n^2} \quad (6a)$$

and

$$G(i\omega) = \frac{n^2 (1 + n^2 - \Omega^2 - 2i\Omega)}{b [(1 + n^2 - \Omega^2)^2 + 4\Omega^2]} \quad (7a)$$

where $\Omega = \frac{n\omega}{b}$.

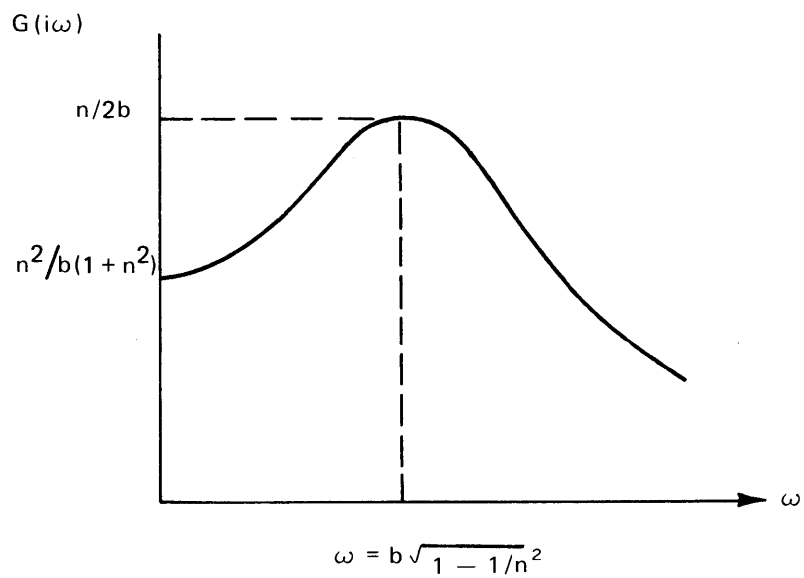
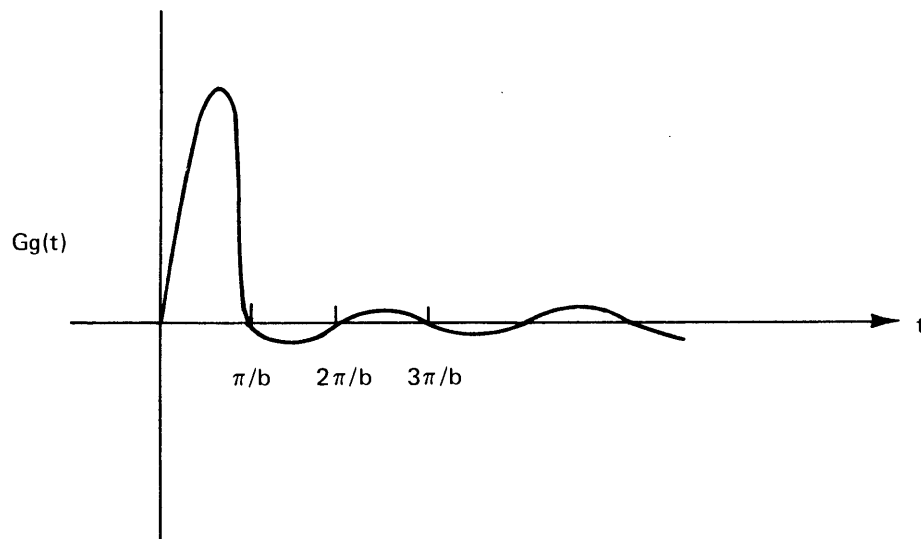


FIGURE 1 THE FORCE FUNCTION AND THE FOURIER TRANSFORM

It follows that

$$|G(i\omega)| = b \left\{ \left[b^2 \left(\frac{1}{n^2} + 1 \right) - \omega^2 \right]^2 + \frac{4b^2 \omega^2}{n^2} \right\}^{-1/2} \quad (8)$$

The maximum value of $|G(i\omega)|$ thus occurs at

$$\omega = b \sqrt{1 - \frac{1}{n^2}} \text{ for } \omega > 0 \quad (9)$$

with a corresponding value, $|G(i\omega)| = \frac{n}{2b}$.

At $\omega = 0$, we have

$$|G(i\omega)| = \frac{n^2}{b(1+n^2)} \quad (10)$$

The ratio of $|G(i\omega)|_{\omega=b\sqrt{1-\frac{1}{n^2}}}$

to $|G(i\omega)|_{\omega=0}$ is thus

$$\frac{|G(i\omega)|_{\omega=b\sqrt{1-\frac{1}{n^2}}}}{|G(i\omega)|_{\omega=0}} = \frac{1}{2} \left(\frac{1}{n} + n \right) \quad (11)$$

Experimental results are needed to determine the spectrum for various sources under various rock types.

The spectrum of the hammer blow or timber impact has the form of Figure 1; thus as n approaches one, the spectrum approaches that assumed by Westinghouse, as depicted in Figure 2 below;

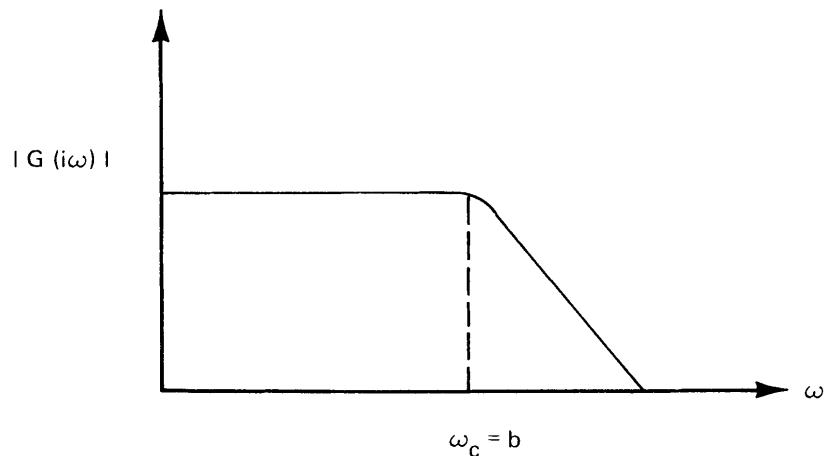


FIGURE 2 SOURCE IMPACT SPECTRUM ASSUMED BY WESTINGHOUSE

i.e., flat from DC to the corner frequency ω_c .

Therefore the radial component of the particle velocity of Equation (2) becomes

$$\dot{u}_r = \frac{Mv (a^2+b^2)^2 \cos\phi}{4\pi b^2 \rho V^2 r} \dot{g}\left[\frac{a^2+b^2}{b} \left(t - \frac{r}{V}\right)\right] e^{-\alpha r} \quad (12)$$

for $a \neq b$

and

$$\dot{u}_r = \frac{Mv (n^2+1)b \cos\phi}{4\pi n^2 \rho V^2 r} \dot{g}\left[\frac{(n^2+1)b}{n^2} \left(t - \frac{r}{V}\right)\right] e^{-\alpha r} \quad (13)$$

for $a = \frac{b}{n}$

For a multilayered model, the radial component of the particle velocity, by virtue of equation (12), becomes

$$\dot{u}_r = \frac{Mv(a^2+b^2)^2 \cos \phi}{4\pi b^2 \rho V_1^2 R} \dot{g} \left[\frac{a^2+b^2}{b} \left(t - \sum_{n=1}^n \frac{r_n}{V_n} \right) \right] e^{-\sum_{n=1}^n \alpha_n r_n} \times T_n(i) \quad (14)$$

$$\text{as } R = r_1 + r_2 + \dots + r_n$$

where V_1 is the compressional wave velocity of the medium in which the source is located, and T_n is the transmission coefficient through the multilayered medium.

IV. NATURE OF THE MINER'S SOURCE

Consider the impact of an elastic rod of length, ℓ , upon a rigid half-space. At the impact, $t = t_0$, $v = v_0$, and $\sigma_0 = v_0 \sqrt{E\rho}$ where t is the time, v_0 is the velocity of the impact, σ_0 is the stress, E is Young's modulus of the rod, and ρ is the density.

Later, for $t > t_0$, if the contact duration is sufficiently long, we have

$$A\rho(\ell-ct) \frac{dv}{dt} + \sigma A = 0 \quad (15)$$

$$\text{as } v = \frac{\sigma}{\sqrt{E\rho}} \text{ and } c = \sqrt{\frac{E}{\rho}}$$

$$\frac{\rho(\ell-ct)}{\sqrt{E\rho}} \frac{d\sigma}{dt} + \sigma = 0 \quad (16)$$

$$\frac{(\ell-ct)}{c} \frac{d\sigma}{dt} + \sigma = 0.$$

Therefore the stress exerted on the rigid medium is

$$\sigma = A' \left(\frac{\ell}{c} - t \right). \quad (17)$$

At $t = t_0$, $\sigma = \sigma_0$

and we have

$$\sigma_0 = A' \left(\frac{\ell}{c} - t_0 \right)$$

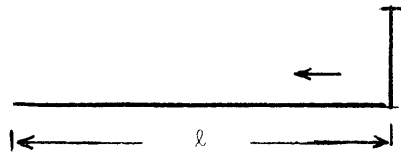
$$A' = \frac{\sigma_0 c}{\ell - c t_0} \quad (18)$$

Hence the stress on the rigid medium is

$$\sigma = \frac{\sigma_0}{\ell - c t_0} (\ell - ct). \quad (19)$$

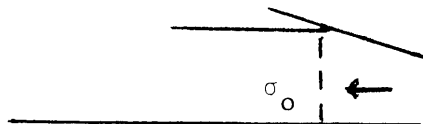
The behavior of equation (19) may be summarized as follows:

(1) at $t = t_0$



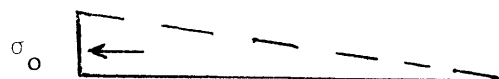
$$\sigma_0 = v_0 \sqrt{E\rho}$$

(2) at $t_0 < t < \frac{\ell}{c}$

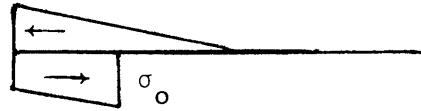


$$\sigma = \frac{\sigma_0 (\ell - ct)}{\ell - ct_0}$$

(3) at $t = t_0 + \frac{\ell}{c}$



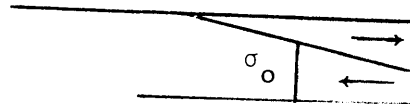
(4) at $t_0 + \frac{\ell}{c} < t < t_0 + \frac{2\ell}{c}$



(5) at $t = t_0 + \frac{2\ell}{c}$



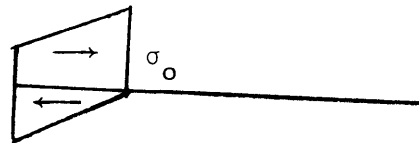
(6) at $t_0 + \frac{2\ell}{c} < t < t_0 + \frac{3\ell}{c}$



(7) at $t = t_0 + \frac{3\ell}{c}$



(8) at $t_0 + \frac{3\ell}{c} < t < t_0 + \frac{4\ell}{c}$



Therefore, if the impact duration is sufficiently long, the longitudinal vibration of the rod is of importance to the stress on the impact medium. It is anticipated that for the case of the impact of an elastic object such as a timber on an elastic medium, the stress should be a function of E_1 , E_2 ,

ρ_1 , and ρ_2 , and furthermore, the initial impact stress might be a function of E_1 , E_2 , ρ_1 , and ρ_2 , as well as of V_0 . This might explain why a timber impact, in addition to its heavier mass, generates lower frequency as well as larger signals than a hammer blow.

V. SIGNAL ATTENUATION

Attenuation of seismic waves is attributed principally to

- (1) geometrical spreading
- (2) energy dissipation
- (3) energy partition due to reflection and transmission at the interfaces of a layered medium.

A. Geometrical Spreading

According to equation (1a), in the far-field the particle displacement is simply inversely proportional to the first power of the distance between the source and the observation point.

B. Energy Dissipation

The dissipation function Q^{-1} for compressional waves propagated in common rocks may be given by (Futterman, 1963)

$$Q^{-1}(\omega) = \frac{1}{2\pi} \left[1 - e^{-4\pi\alpha V/\omega} \right], \quad (20)$$

where α is the attenuation coefficient.

For small dissipation such that $\frac{4\pi\alpha V}{\omega} \ll 1$,

equation (20) may be approximated by

$$Q^{-1}(\omega) \approx \frac{2\alpha V}{\omega}, \quad (21)$$

so that the attenuation coefficient in terms of Q^{-1} is

$$\alpha \approx \frac{\pi f}{VQ}^* \quad (22)$$

where f is the frequency in Hz.

*This expression differs by a factor of 2 from that given in the Westinghouse Final Report (1971), Section II, p. D-16.

Therefore, the attenuation coefficient is a function of ω as shown in Figure 3. Basic physical considerations indicate that the attenuation should disappear at some low frequency cut-off ω_0 , which has accordingly been included in Figure 3, although reliable estimates of its values are not yet available.

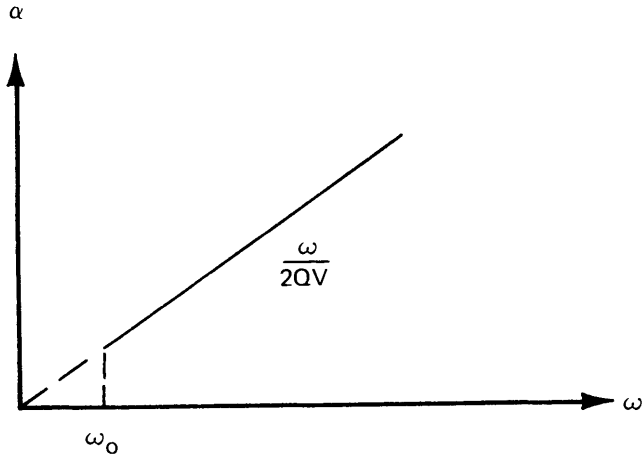


**FIGURE 3 ATTENUATION COEFFICIENT VERSUS FREQUENCY
WITH A LOW-FREQUENCY CUT-OFF**

Valuable information on the value of Q for Eastern Coal Province, Southern Appalachian field, Interior Coal Province, and Rocky Mountain coal regions is given by Westinghouse (Final Report II, p. D16-18).^{*} Average values of Q for various rock types are approximately given in (without specifying the frequency range) Table 1.

TABLE 1

| <u>AVERAGE VALUES OF Q</u> | |
|-------------------------------------------|----------|
| <u>Rock Type</u> | <u>Q</u> |
| Cap rock | 50 |
| Dolomite | 200 |
| Limestone | 120 |
| Marlstone, sandstone, shale and siltstone | 50 |

^{*} Ibid.

Since the coal region is generally covered by weathering layers and soils, the following are values of Q for soils for compressional waves in the frequency range of interest (Table 2):

TABLE 2
Q's FOR TYPICAL WEATHERING LAYERS

| Formation | Frequency Range | Q | Source |
|----------------------|-----------------|----|------------------------|
| Pottsville sandstone | 100-900 Hz | 7 | Collins and Lee (1956) |
| Pierre shale | 50-450 Hz | 23 | McDonal et al. (1958) |

The average values of α are approximately (Table 3):

TABLE 3
AVERAGE VALUES OF ATTENUATION COEFFICIENT, α

| Rock Type | Compressional wave velocity ft/sec | Q | Frequency Hz | α nepers/ft |
|-----------------|------------------------------------|-----|--------------|-----------------------|
| Dolomite | 16,000 | 200 | 100 | 9.82×10^{-5} |
| Limestone | 14,000 | 120 | 100 | 1.87×10^{-4} |
| Sandstone | 8,000 | 50 | 100 | 7.85×10^{-4} |
| | 10,000 | 50 | 100 | 6.28×10^{-4} |
| Weathering zone | 4,000 | 15 | 100 | 5.24×10^{-3} |
| | 2,000 | 10 | 50 | 7.85×10^{-3} |

C. Energy Partition

The fraction of the energy incident in a plane wave upon a plane interface, separating two semi-infinite media, that is carried away in each of the reflected and refracted waves, can be directly calculated on a computer. Among various authors, e.g., Costain et al. (1963), McCamy et al. (1962)*, etc., Nafe (1957) has expressed the Knott equations (1899) in common coordinate system for the four separate problems of incident P (or SV) waves from either side of the interface in a symmetrical form, which is convenient for numerical calculation.

*There is an error in sign in McCamy et al.'s (1962) paper.

Consequently, their results are incorrect.

Referring to Figure 4, if the incident waves are assumed to have unit amplitude, the sixteen equations for the amplitudes may be expressed as the matrix product:

$$MX = N \quad (23)$$

where

$$M = \begin{pmatrix} 1 & \tan\sigma & -1 & \tan\sigma' \\ -\tan\delta & 1 & -\tan\delta' & -1 \\ \mu q & -2\tan\sigma & -\mu'q' & -2\mu'\tan\sigma' \\ 2\mu\tan\delta & \mu q & 2\mu'\tan\delta' & -\mu'q' \end{pmatrix} \quad (24)$$

$$X = \begin{pmatrix} (P,P) & (P,S) & (P,P') & (P,S') \\ (S,P) & (S,S) & (S,P') & (S,S') \\ (P',P) & (P',S) & (P',P') & (P',S') \\ (S',P) & (S',S) & (S',P') & (S',S') \end{pmatrix} \quad (25)$$

$$N = \begin{pmatrix} -1 & \tan\sigma & 1 & \tan\sigma' \\ -\tan\delta & -1 & -\tan\delta' & 1 \\ -\mu q & -2\mu\tan\sigma & \mu'q' & -2\mu'\tan\sigma' \\ 2\mu\tan\delta & -\mu q & 2\mu'\tan\delta' & \mu'q' \end{pmatrix} \quad (26)$$

where μ' and μ are rigidities, and q and q' are equal to $(\tan^2\sigma - 1)$ and $(\tan^2\sigma' - 1)$, respectively.

The notation of (P,S') or (P',P) refers to the outgoing wave by the first letter, and the incident wave by the second letter.

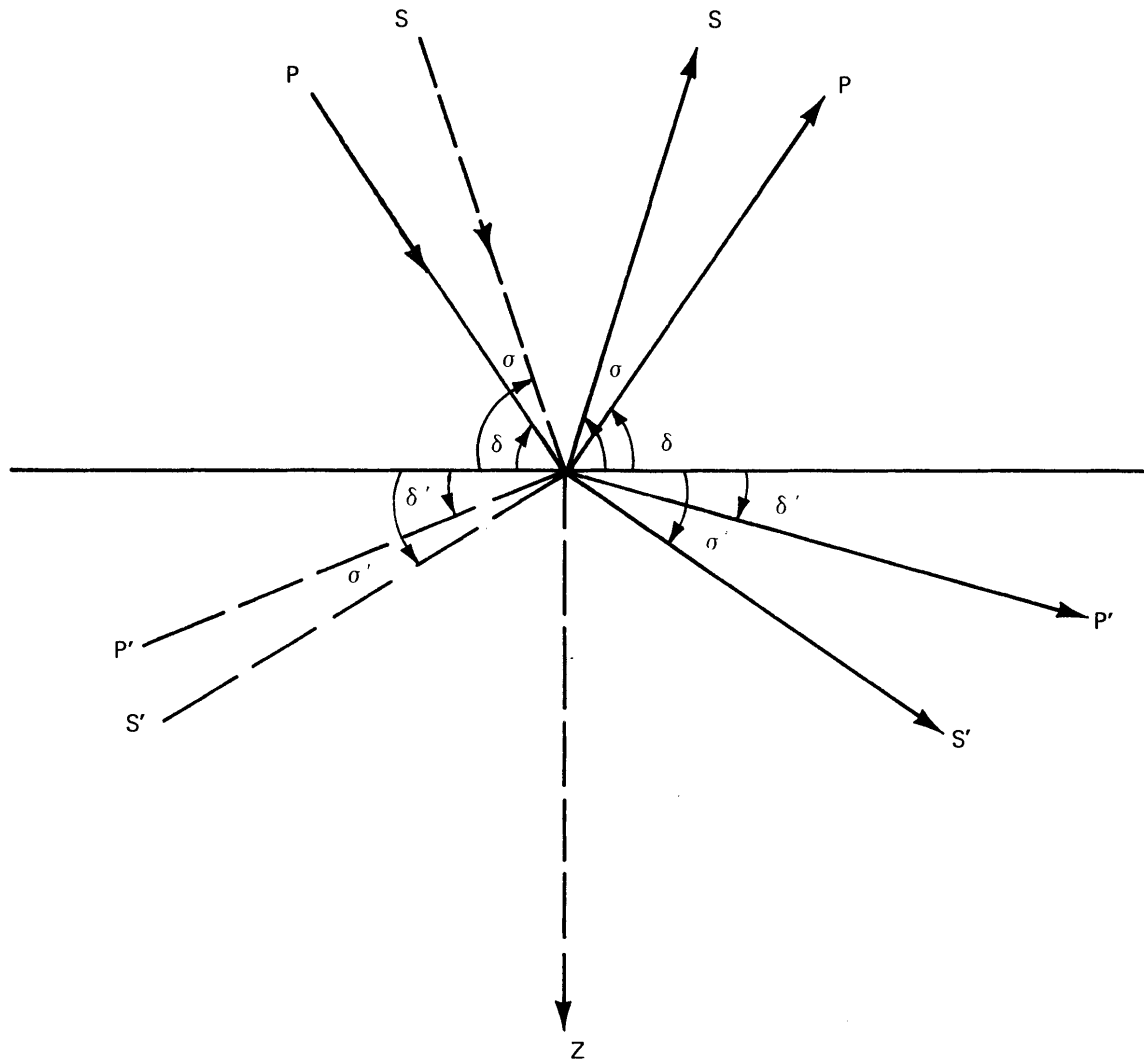


FIGURE 4 FOUR INCIDENT PLANE WAVES ARE SHOWN APPROACHING A PLANE INTERFACE. ANY ONE OF THESE PRODUCES FOUR OUTGOING WAVES, P, S, P', S'. THE ANGLES OF EMERGENCE FOR SHEAR WAVES ARE σ AND σ' , AND FOR COMPRESSIONAL WAVES, δ AND δ' . THE UPPER MEDIUM IS UNPRIMED. (After Nafe, 1957).

The cases for the velocity ratios of 1:2, 1:2.5, and 1:3, and the densities 2.3 and 2.8, which are directly applicable to the present requirements of a weathering zone in contact with sandstone or limestone, are shown in Figure 5 for the range of incident angles from 0 to 60°.

The present results can be easily applied to the case of plane waves in a multilayered medium used to represent the geological structure of a coal mine region. A similar analysis was performed by Haskell (1962) in treating crustal reflection of P and S waves in a layered medium. However, the problem of calculating reflection and transmission coefficients for a point source located in a layered medium requires further investigation.

VI. DISTORTION OF SEISMIC WAVE FRONT FOR AN IMPACT SOURCE IN A MINE OPENING

Evidently, the assumption of a simple force in an infinite medium for a hammer blow (or a timber strike) on either the roof or the ribs of a mine opening is not adequate. The radiation pattern generated by a simple force in an infinite medium is spherical, whereas that of a simple force impacted on a cavity has a distorted spherical shape. Figures 6a and 6b give a comparison of these two wave front patterns.

Because of the general complexity of a mine section including a grid of tunnels, it is virtually impossible to represent the wave front generated by a source under actual mine conditions. Fortunately, the wave length we are dealing with is generally large in comparison with at least the cross-section of an opening. Unless the impact is on the floor, the approximate spherical wave front of the impact on either the roof or the rib would not be significantly distorted as it impinges on the surface, as shown in Figure 6b.

It must be cautioned, however, that when the impact is on the floor the wave front is severely distorted. The degree of its distortion naturally depends upon the dimensions of the opening as shown in Figure 7; for a floor impact the first arrival of P waves on the surface should be expected to have a considerable time delay. Figures 8, 9 and 10 represent the wave distortion in sections A-A' and B-B' for a three-dimensional representation of a long tunnel with impact on the roof, the rib and the floor.

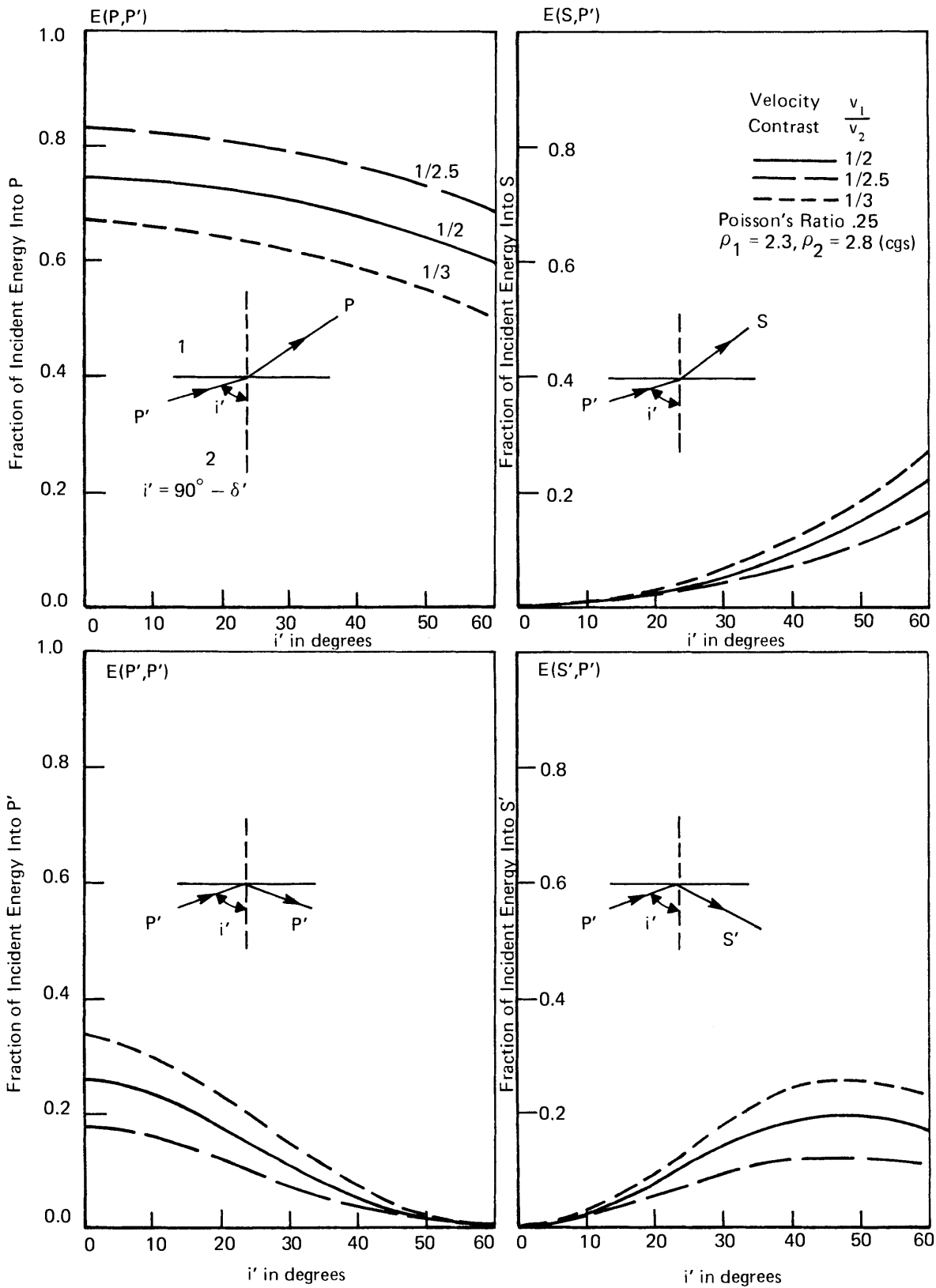
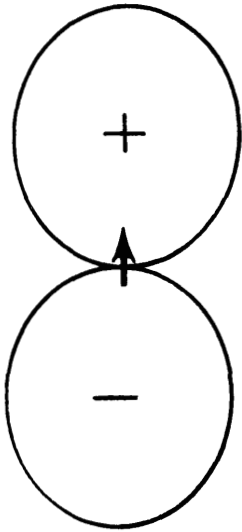
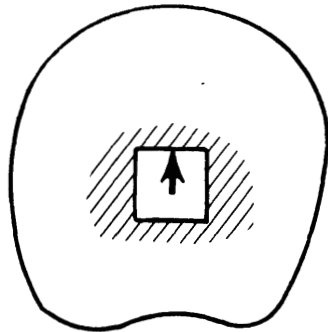


FIGURE 5 FRACTION OF INCIDENT ENERGY CARRIED AWAY IN REFRACTED (P, S) AND REFLECTED (P', S') WAVES



(a) A simple force in an infinite medium



(b) A simple force in a mine opening

FIGURE 6 RADIATION PATTERNS OF A SIMPLE FORCE IN (a) AN INFINITE MEDIUM AND (b) A MINE OPENING

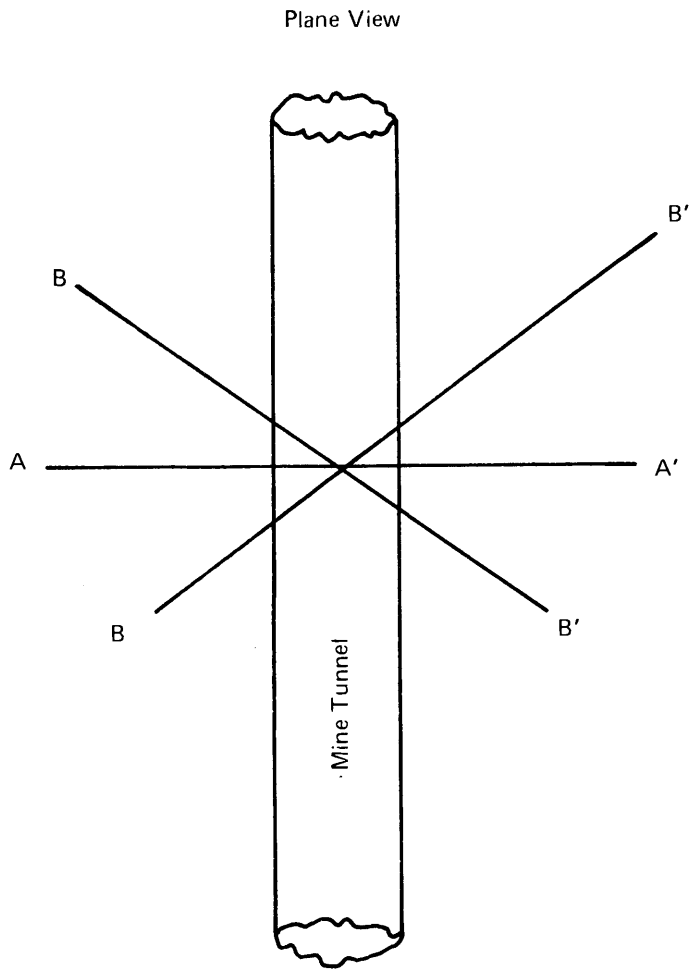


FIGURE 7 PLANE VIEWS FOR MINE TUNNEL

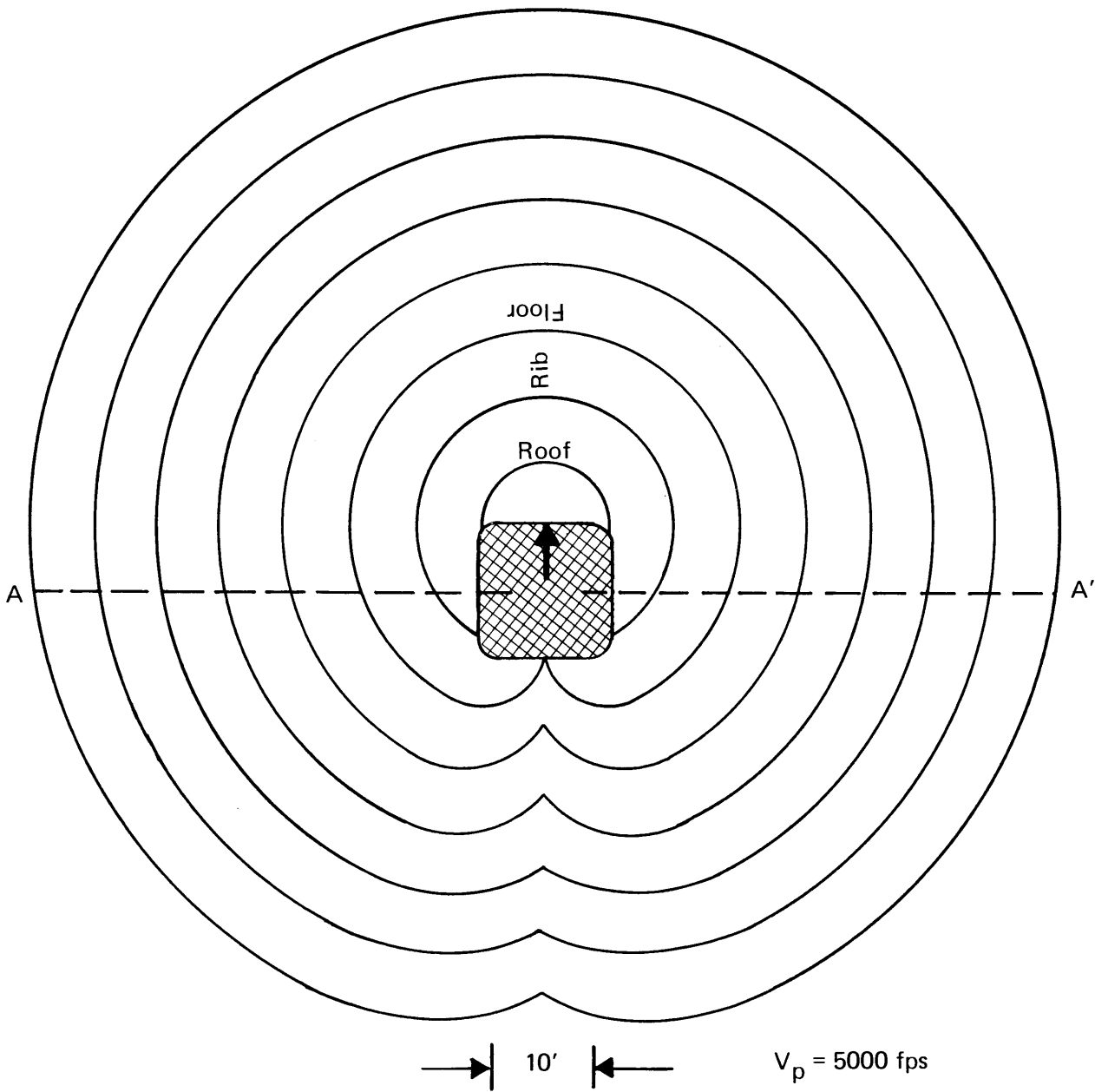
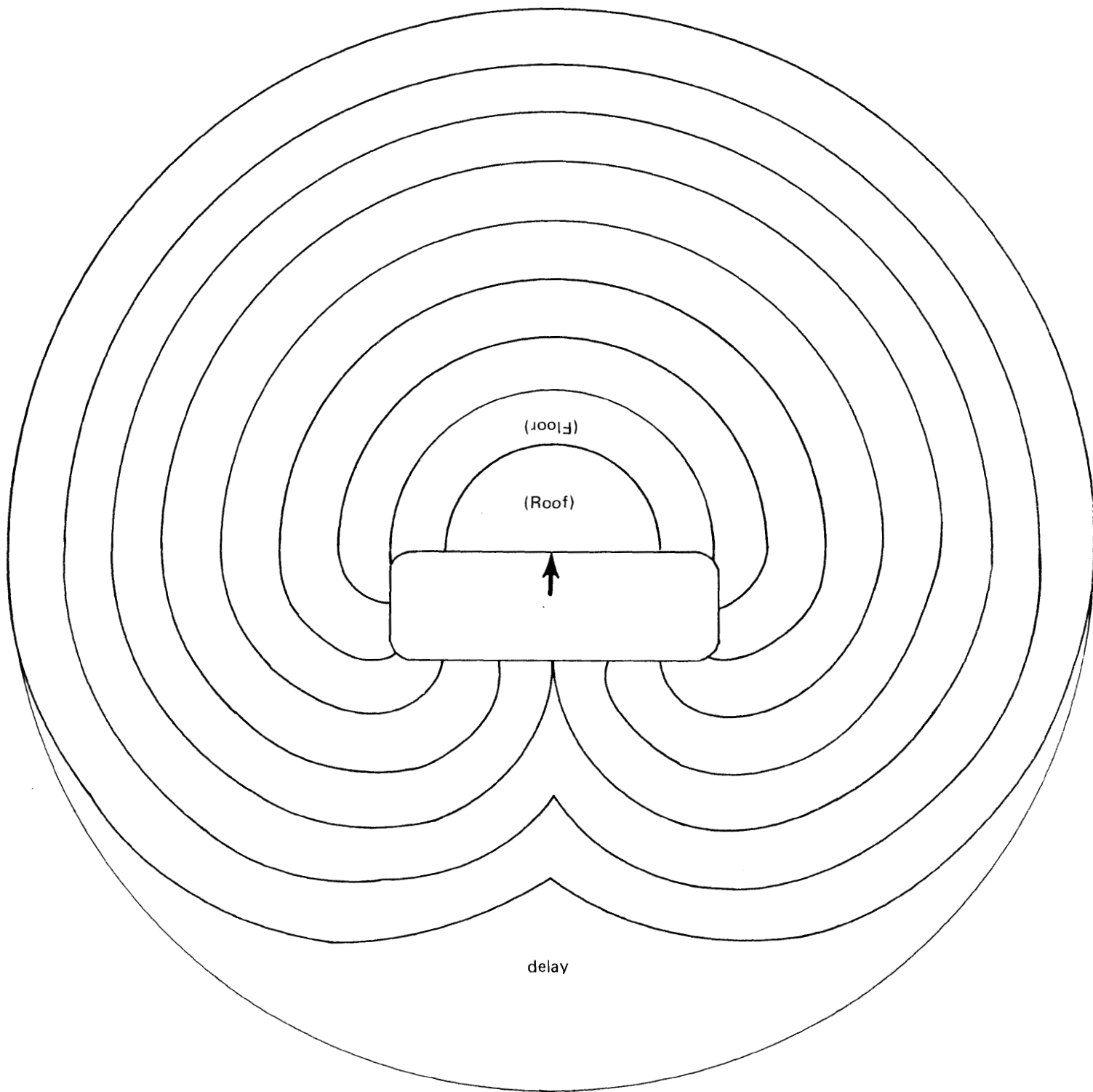


FIGURE 8 DISTORTED WAVE FRONTS OF A VERTICAL SECTION A-A'



$V_p = 5000$ fps

← 10' →

FIGURE 9 DISTORTED WAVE FRONTS OF A VERTICAL SECTION B-B'

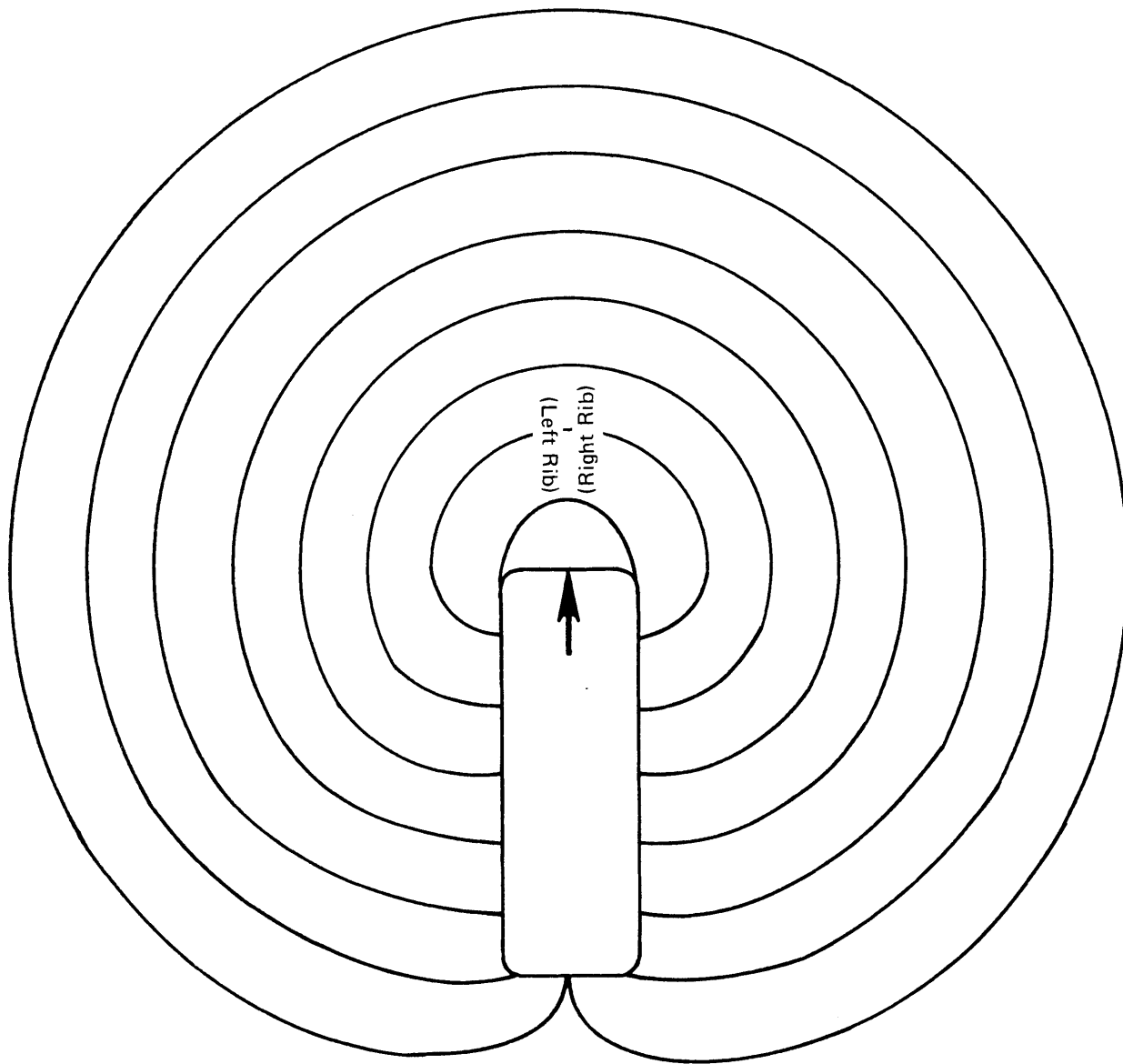


FIGURE 10 **DISTORTED WAVE FRONTS OF A VERTICAL SECTION B-B' FOR AN IMPACT ON RIB**

VII. THEORETICAL ESTIMATION OF THE SIGNAL LEVEL AS A FUNCTION OF RANGE

Neglecting the effect of noise on the signal, the particle velocity may be approximately calculated by Equation 13. The remaining problem is then to estimate the efficiency of energy conversion from mechanical impact to seismic-wave transmission, which naturally depends on the dimension, elastic properties and the velocity of the impact body, and the stress thereby induced in the impact medium. Such an estimation, without controlled experimental data, involves a high degree of uncertainty. We will assume a 70% effective elastic collision as a hammer strikes the rock in a mine opening.

As a specific example, we use the models of Figure 11, which are close to the geological model at Imperial Mine (Westinghouse Final Report II,*Figure 3.1-3, p. 92)

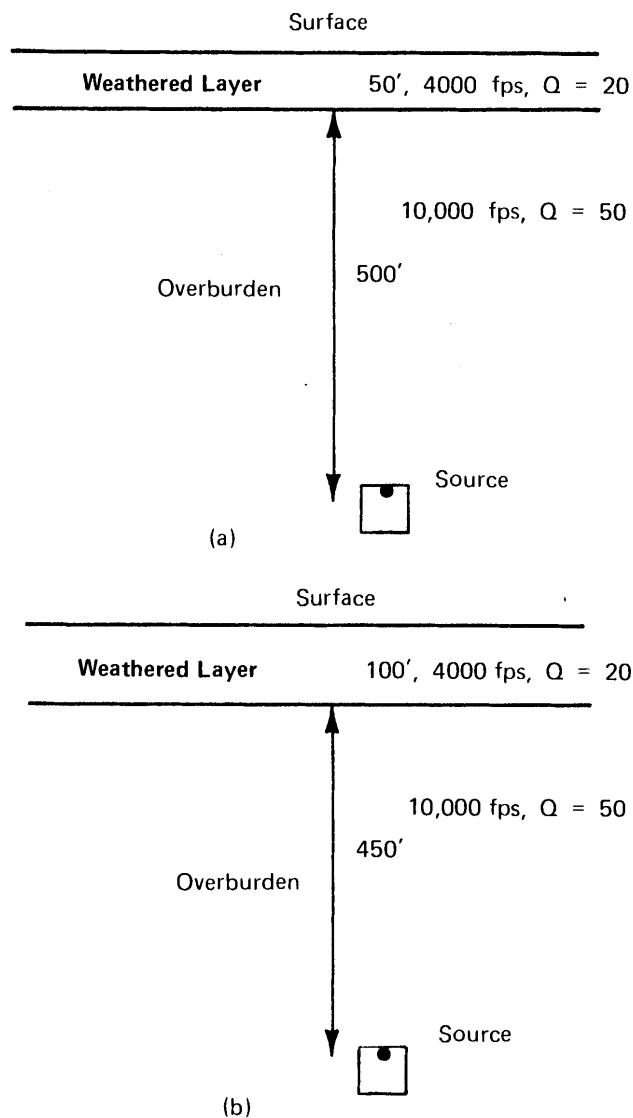


FIGURE 11 MODELS FOR ESTIMATING SIGNAL LEVELS ON THE SURFACE

* Ibid.

and the values of

M = a 10-lb sledge hammer; a 40-lb timber

v = 16.1 ft/sec for hammer; 11.5 ft/sec for timber

$\rho = 2.67 \text{ gm/cm}^3$ for 10,000 ft/sec half-space

Taking into account all the factors of the geometrical spreading, energy dissipation, and energy partition at the interface as described in the preceding section, the vertical component of the peak-to-peak particle velocity on the surface of the model is given in Figure 12 for the cases of 50 Hz and 100 Hz as a function of slant range for a hammer blow and a timber impact.* The up- and -down-link experimental data for the frequency range of 70 to 83 Hz (Table 2.5.3-1, Westinghouse Field Report 8)† at Copper Queen is also plotted in the Figure. The rates of decay for the theoretically calculated and the experimental data agree rather closely. The theoretical magnitude of the peak-to-peak particle velocity seems somewhat overestimated for a hammer blow, as the source used at Copper Queen is a thumper for uplink and a timber for downlink. This is an unfair comparison, as the geological models vary between the theoretical situation and that of Copper Queen, since the geology at Copper Queen is complicated by faults and irregular distribution of alluvial materials. Nevertheless, it does provide evidence of the applicability of such a crude approximation in theoretical calculations.

VIII. DEVELOPMENT OF LOW-FREQUENCY SEISMIC SOURCE FOR THE DETECTION OF SURVIVING MINERS

Present seismic detection methods are handicapped because only very weak signals can be generated by a trapped miner with available tools such as a sledge hammer or a timber. The detectability of a trapped miner should be greatly enhanced if a suitable low-frequency source can be developed. Since the option of what a miner may be able to carry is rather limited, it appears not altogether unreasonable to consider a permanent installation of a mechanical source generator of the simplest kind. An electrically or electronically driven transducer is ruled out because of its requirement for either sophistication or power. It seems that heavy-weight simple pendulums can be installed in strategic locations in an actual mine section. As the signal strength for an impact source is directly proportional to the mass of the impact body, a "lead" sphere type of simple pendulum may be appropriate. Such installations cost relatively little. The support of the pendulum can be anchored either to the roof or to the rib as

* A relatively large value of n has been assumed, so that the source signal strength (see Figure 1) is noticeably higher at 100Hz than 50Hz.

† Westinghouse Contract H0210063 with Bureau of Mines.

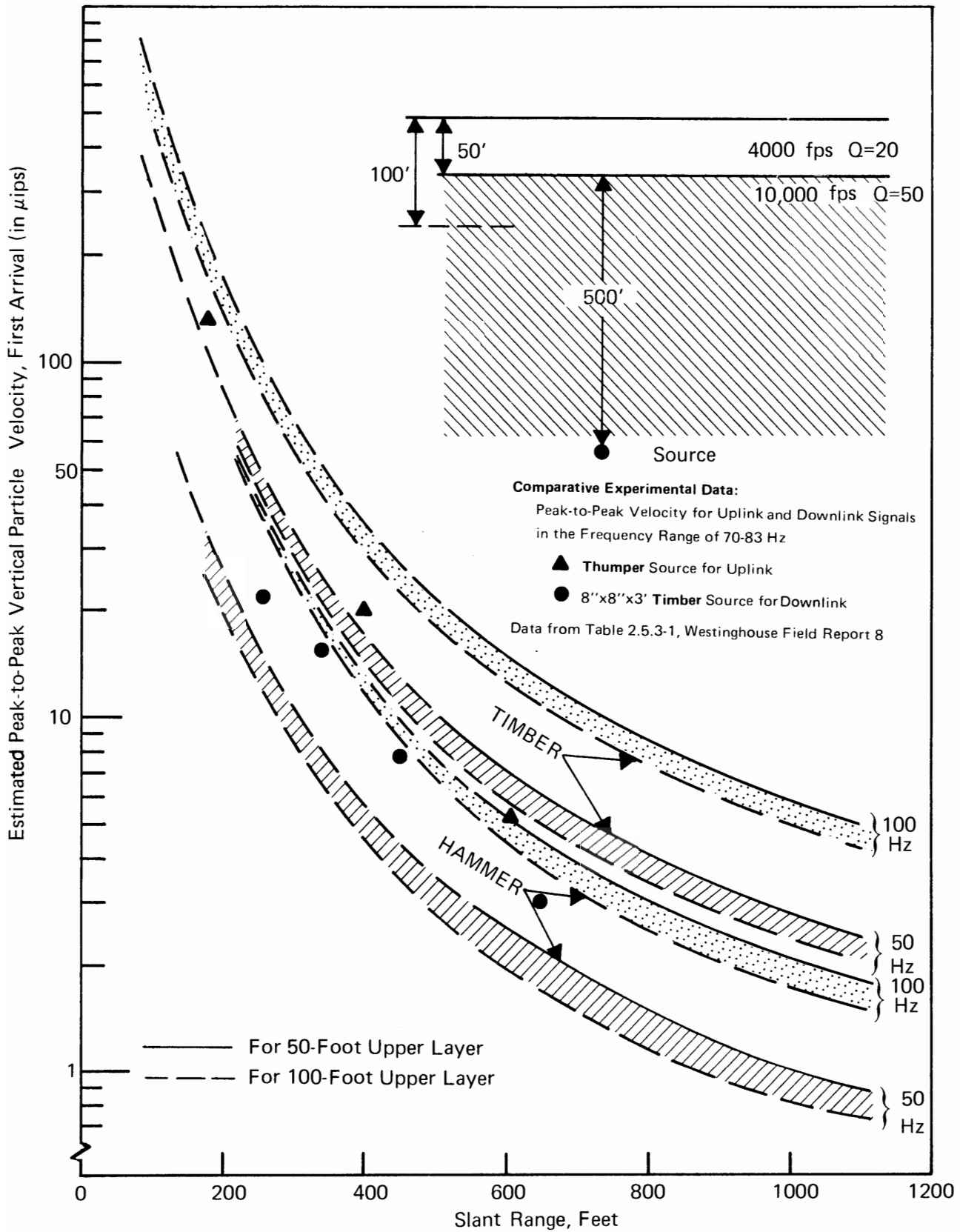


FIGURE 12 ESTIMATED PEAK-TO-PEAK VERTICAL PARTICLE VELOCITY FOR THE FIRST P-WAVE ARRIVAL (BASED ON THEORETICAL CONSIDERATIONS)

the following diagram (Figure 13) illustrates.

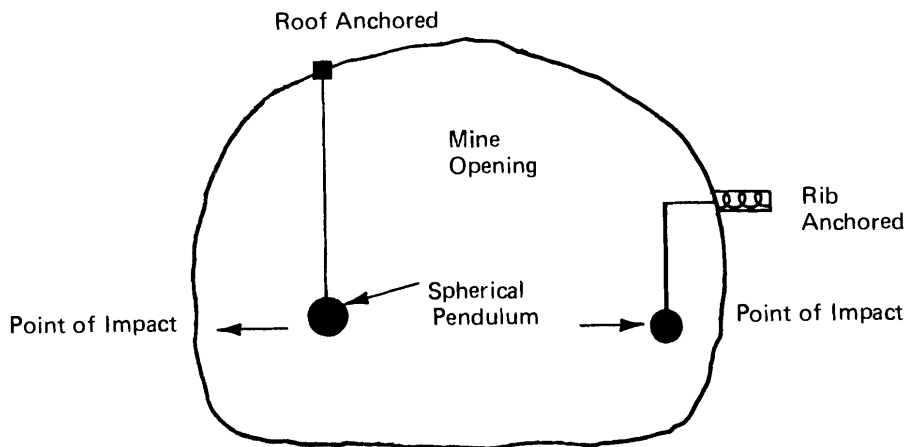


FIGURE 13 PERMANENT INSTALLATION OF A PENDULUM

The signal can be generated repeatedly without great effort on the part of a trapped miner. Furthermore, the particle velocity is also directly proportional to the impact velocity. If the impact of a timber is comparable to that of a hammer blow, the magnitude of the particle velocity due to the impact of a lead sphere would be about an order of magnitude higher than that due to a 10-lb sledge hammer blow. If the impact is made on a floor filled with soft earth material or in a coal seam, a coupler may be installed at the point of impact to enhance the conversion of mechanical energy into seismic energy without much energy loss in permanent deformation of the medium. Experimental results of impact on sand and sand-silt clay show a great deal of promise for eliminating energy loss from plastic deformation and heat generation (Appendix A and Mereu et al. (1963)).

For the initial detection of surviving miners in a disaster-struck mine, a positive, immediately identifiable signal of yes/no would be of great value for subsequent operation. Since the high frequency components of a signal attenuate rapidly in earth materials, particularly in weathering layers such as alluvium and soil, as is clearly demonstrated in Figure 14, a "low-frequency" source is preferred, i.e., with a peak frequency in the neighborhood of 10 Hz. A hammer

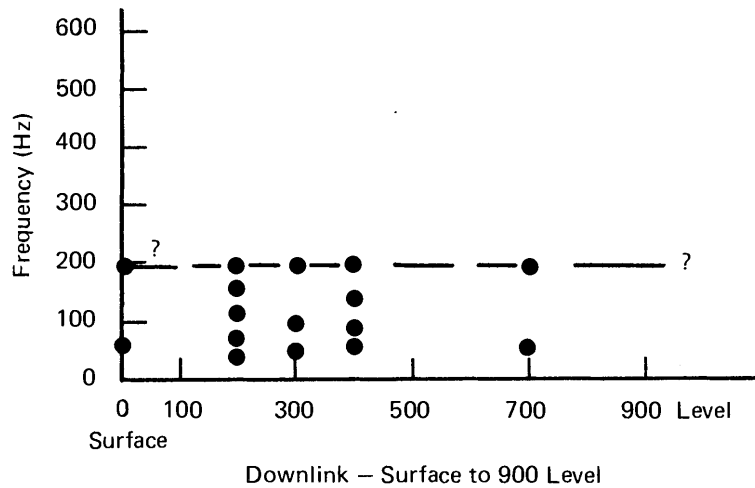
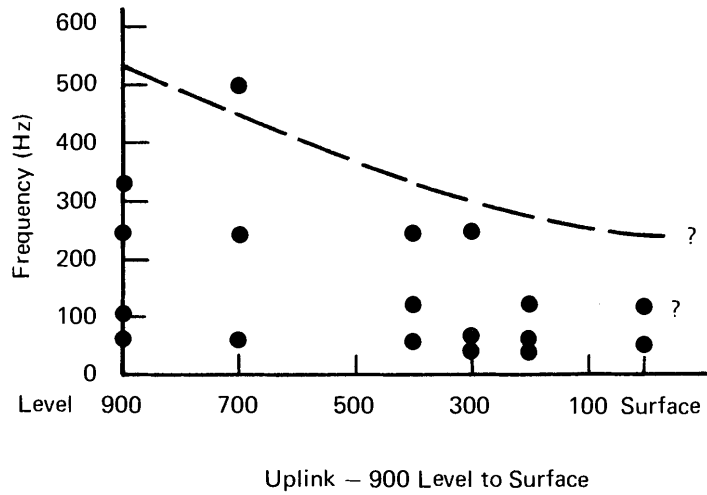


FIGURE 14 ATTENUATION OF HIGH FREQUENCIES THROUGH WEATHERING LAYERS AS DEDUCED FROM PLOTS 38 AND 39 OF REPORT 8, COPPER QUEEN

or a lead sphere with a spring mount as shown in Figure 15 promises to generate lower frequencies of this order. Future efforts toward developing a low-frequency source could be very worthwhile.

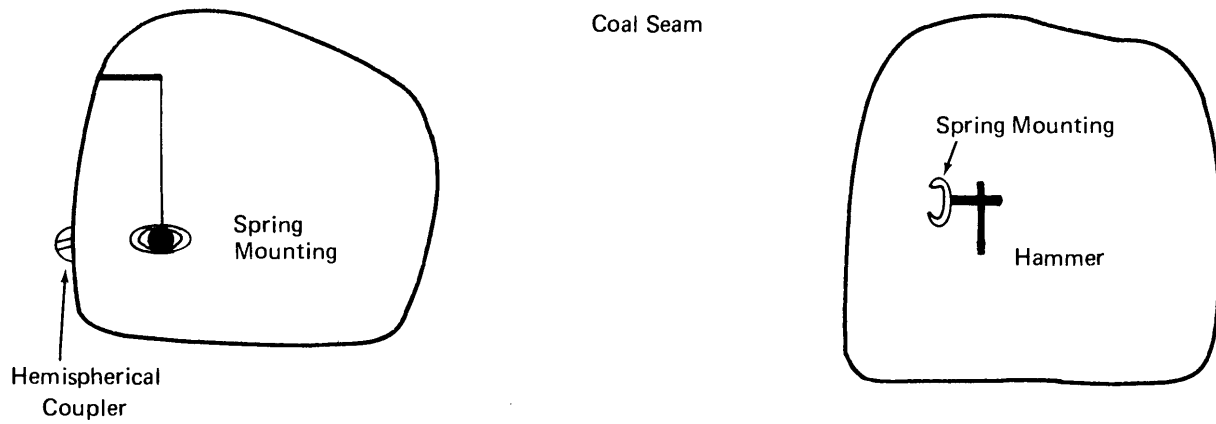
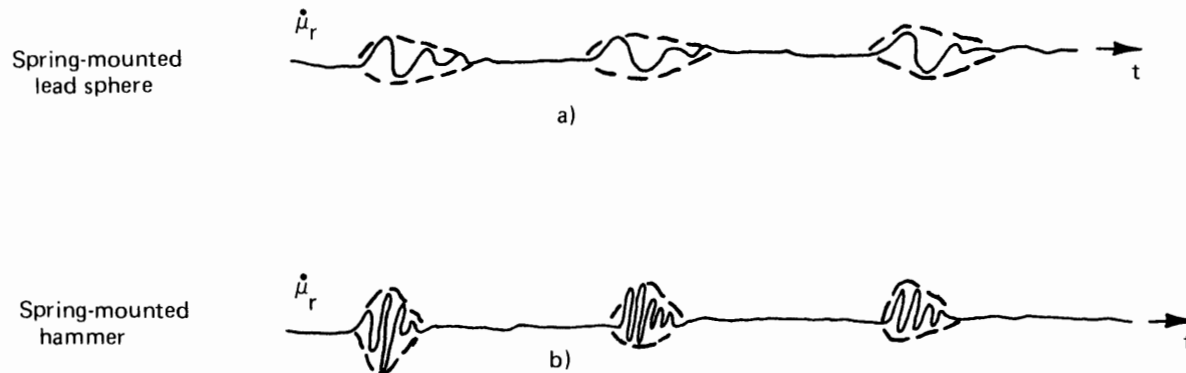


FIGURE 15 EXAMPLES OF LOW FREQUENCY SOURCES

In the time domain, a repeated low-frequency signal received on the surface should have the following forms (Figure 16).



**FIGURE 16 REPEATED LOW-FREQUENCY SIGNALS
AS RECEIVED ON THE SURFACE**

It should be of great value to analyze the envelopes of the signals in the frequency domain, instead of the actual signals themselves. The spectra of the time series of these envelope signals should contain the low frequency energy of repeated sources. If the signals are sufficiently strong, their envelopes could themselves offer direct visual identification of the presence of surviving miners. Once surviving miners have been successfully detected, a down-link signal can be sent to tell survivors to use a high-frequency source with a shorter range of transmission for the purpose of accurate location.

IX. FUTURE INVESTIGATIONS

- (1) Wave diffraction and scattering of an impact source on a face of a cylindrical cavity.
- (2) The impact of an elastic object on an elastic medium.
- (3) Spectrum of the source, sufficiently far from the source to determine $G(i\omega)$ as a function of frequency. This information should be of great value for more accurate determination of the source strength, as it is virtually impossible to determine the source strength near or at the source because the conversion of mechanical energy to seismic energy remains a difficult problem.

X. REFERENCES

1. Collins, F., and C. C. Lee (1956). Geophysics 21, 16-39.
2. Costain, J. K., K. L. Cook, and S. T. Algermissen (1963). Bull. Seism. Soc. Am. 53, 1039-1074.
3. Futterman, W. I. (1962). J. Geophys. Res. 67, 5279-5291.
4. McCamy, K., R. Meyer, and T. J. Smith (1962). Bull. Seism. Soc. Am. 52, 923-956.
5. McDonal, F. J., F. A. Angona, R. L. Mills, R. L. Sengbush, R. G. Van Nostrand, and J. E. White (1958). Geophysics 23, 421-439.
6. Mereu, R. F., R. J. Uffen, and A. E. Beck (1963). Geophysics 28, 531-546.
7. Nafe, J. E. (1957). Bull. Seism. Soc. Am. 47, 205-219.
8. White, J. E. (1965). Seismic Waves: Radiation, Transmission and Attenuation, McGraw Hill, New York 302 pp.
9. Knott, C. G. (1899). Phil Mag. 48, 64-97
10. Coal Mine Rescue and Survival System, Vol. II, Communications/Location Subsystem, Westinghouse Final Report, Bu Mines Contract H0101262, Sept., 1971.
11. Haskell, N.A. (1962), J. Geophysics Res. 67, 4751-4759.
12. Westinghouse Field Report No. 8, Copper Queen Mine, Bisbee, Arizona, January 1972, Contract H0210063.

APPENDIX A

USE OF A COUPLER IN THE CONVERSION OF
IMPACT ENERGY INTO SEISMIC ENERGY

Mereu et al (1963) presented an interesting paper on the efficient transfer of impact energy into seismic energy in soil-covered areas by means of a falling weight-coupler system. This concept is equally applicable to the present problem of impact on a coal seam or on a floor generally covered with rock debris or soils. Through their theoretical and experimental model studies on sand and clay-silt sand, the authors concluded that for compressional waves:

- (1) A coupler such as a plastic steel hemisphere embedded in the medium at the impact point can increase the amplitude of the seismic output by reducing plastic deformation at the point of impact, i.e.,

$$A \sim M^{2/3} V_c \tag{A1}$$

where A is the amplitude of the seismic signal, M the mass of the coupler, and V_c the maximum velocity of the coupler.

- (2) The seismic energy is not proportional to the source energy.

APPENDIX B

QUADRATURE WEIGHTING METHOD FOR MINER LOCATION ARRAYS*

In principle it is possible to cope with the problem of bias in location estimation by using a different station weighting procedure than that adopted in Part Three. The stations in each quadrant are considered in separate groups. When an approximate location has been determined, the residues for each station in a group are computed, and obviously "abnormal" stations are rejected. Subsequently, an average residue is calculated as

$$\bar{R} = \frac{1}{N} \sum_i R_i \quad (B1)$$

where N is the number of stations in the group.

It is assumed that residue values follow a Gaussian distribution about this mean value, to which a weighting factor of unity is assigned. Finally a weighted residue is computed for each station by using a weighting factor which corresponds to the position of the original residue on the Gaussian distribution.

Appropriate quadrants for the miner location problem might be as follows (Figure B1).

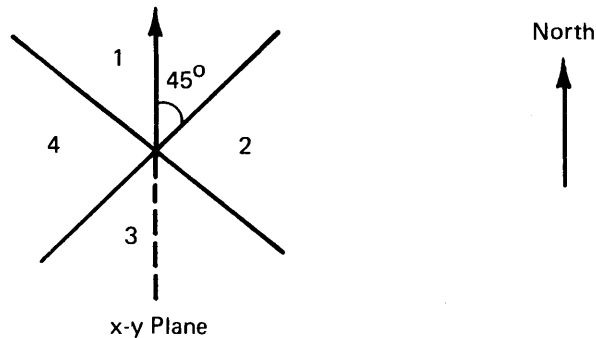


FIGURE B1 QUADRANT GEOMETRY

*This method has been in common use at the Lamont Geological Observatory for earthquake focus relocations (Kuo et al.).